

# Direct Extraction of Complementary RF Design Information from Active Load- Pull Measurements

**Author: Azam Al-Rawachy**

Software Department, University of Mosul, Mosul, Iraq

*Azzam.esam@uomosul.edu.iq*

## ABSTRACT

*This paper reveals the limitation of load-pull measurements and the lack of providing relevant design data in the active load-pull system. To observe the device's stability during active load-pull measurements, tickle tones can be exploited to obtain a better idea of the loads being measured. With tickle-tones set to -20dBc, the required data could be collected successfully without distorting main tone measurements for stability and gain calculations. To provide design-relevant gain parameters in active load-pull systems, we used this approach to measure all four travelling waves simultaneously under the large-signal regime. Thus, these systems can be directly used for RF power amplifier design by transforming them into relevant design tools.*

**Keywords:** load-pull measurements, Tickle-tones, stability.

## 1. INTRODUCTION

There have been many studies in recent years regarding the use of load-pull techniques to characterize devices under test (DUT) in large signal regimes [1]–[3]. These techniques are helpful for determining appropriate matching impedance values in non 50Ohm regions. When the optimum load impedance is determined, useful figures of merit can be extracted from the DUT, such as output power, efficiency, gain, and power-added efficiency. Load-pull systems are limited by the inability to provide additional information about stable or unstable loads, which could lead to an unstable Power Amplifier (PA).

The seamless integration of tickle-tones into active load-pull allows for the transformation of such systems into a direct design tool. This can be achieved by utilizing a receiver with inherent instantaneous bandwidth and choosing appropriate tickle-tone magnitudes and phases to provide a complete set of small-signal data of the device and impedance mismatches at its terminals. The same measurement data can then be used to provide complimentary information alongside the behavioural model. For instance, four tickle-tones enable the monitoring of the stability of the DUT at each load point under large signal excitation and can be used for gain figure calculation.

This paper demonstrates that inclusion of tickle-tones in measurement systems with an instantaneous bandwidth can be done without increasing the number of acquisitions. Without this the measurements can suffer from increased frequency switching of receivers, which slows down measurements.

## 2. GENERAL PRESENTATION OF LOAD-PULL MEASUREMENTS

A similar setup has previously been published in non-linear measurement systems with PXIe modules [4]. As shown in Fig.1, the power and efficiency contours for the large-signal stimulus around the maximum optimum load are coloured in blue and red, respectively.

This data is still inadequate from RF design point of view as they do not imply whether the selected loads are stable or not. Furthermore, usually, RF designers used 50Ohm load to check the stability

(in grey) which is, in reality, inaccurate way as the power and the load impedance are different. The measurement system was developed to be able to provide a complementary data during the measurements by injecting a tickle tone at each port with different frequency spacing for testing the stability analysis.

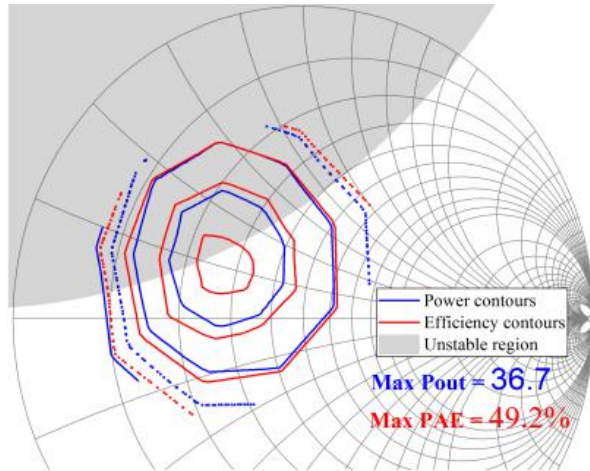


**Fig 1: Power and efficiency contours at optimum load.**

### 3. Tickle-Tones Measurements in Active Load-Pull System

Numerous studies have been conducted about load-pull techniques and their application in characterizing large-signal devices in recent years [5-7]. Using these techniques, it is possible to determine the correct matching impedance for non-50 Ohm circuits. By measuring load impedance, it is possible to obtain useful figures of merit from DUTs, such as output power, efficiency, gain, and power-added efficiency. In active load-pull measurements, it is difficult to identify information such as gain in real time because  $S_{12}$  and  $S_{22}$  are inaccurate since the  $b_2$  signal is directly affected by the input signals  $a_1$  and  $a_2$ . A complete load-pull measurement can yield accurate S-parameters from a set of load-pull data. Calculating accurate gain figures would only be possible then.

When measuring the load-pull, two additional tickle-tones with different frequency spacing are introduced to provide complementary information to RF designers. Through tickle tones, transistor S-parameters about a large signal operating point can now be computed in real-time, based not just on the DC bias point but also on the input stimulus level and load impedance of a large signal operating point. It is also possible to measure various system

impedances. Using this additional information, large signal load-pull measurements can be performed to calculate parameters, such as stability circles. In this way, it is possible to monitor the stability of the DUT under large signal excitation at each load point. Additionally, by measuring small-signal S-parameters, it is possible to calculate the source impedance (gamma source ( $\Gamma_S$ )) at the input. By using this information, it is possible to calculate different gain figures for different sources that are mismatched with regard to the source, such as the available gain  $G_A$  and the transducer gain  $G_T$ .

### 3.1 Tickle-Tone Verifications Under Large-Signal Input

In Figure 2, two tickle-tones  $T_1$  and  $T_2$  at different frequencies are simultaneously injected into the device's two ports as well as the fundamental signals  $a_{1F}$  and  $a_{2F}$  to determine all four S-parameters of the DUT.

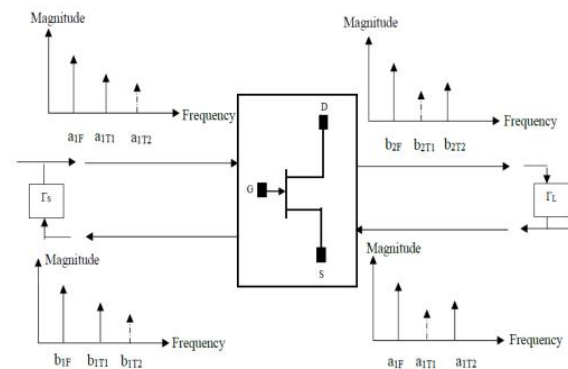


**Fig 2: Incident reflected tones for device measurements.**

By choosing frequencies that are offset from the fundamental frequency and tickle tone frequency, no mixing terms will interfere with the injected three frequencies. A sufficient distance is maintained between the tones so that the S-parameter measurements accurately reflect the DUT's performance at the fundamental frequency. In Figure 2, because of non-ideal source and load impedances, all four S-parameters can be measured at the same time using the relationships described below.

$$S_{11} = \left. \frac{b_{1T1}}{a_{1T1}} \right|_{a_{2T2}=0} \quad S_{21} = \left. \frac{b_{2T1}}{a_{1T1}} \right|_{a_{2T2}=0} \quad 1$$

$$S_{22} = \left. \frac{b_{2T2}}{a_{2T2}} \right|_{a_{1T1}=0} \quad S_{12} = \left. \frac{b_{1T2}}{a_{2T2}} \right|_{a_{1T1}=0} \quad 2$$

The tickle-tone measurements were also verified using a thru calibration standard with the main-tone present. In the first study, the main-tone frequency was set to 250kHz and the tickle-tone frequency to 100 kHz, while the injection power of the  $a_1$  and  $a_2$  signals at 24.6dBm was kept constant and the tickle-tone power swept from 0dBc to -80dBc.

Starting at -70dBc offset, Figure 3 shows the resulting deviation in phase and magnitude. Based on these measurements, the measurement system has a dynamic range of -70dBc. Additionally, it is important to determine the maximum power offset that does not significantly impact the performance of large signals when determining the available power range for characterization of active devices. Tickle tones should not affect main-tone measurements while still providing sufficient accuracy for determining S-parameters and impedance.

An additional experiment evaluated tickle tone measuring at IDQ = 11mA and VDS = 28V using a deep class-AB bias point at  $\Gamma_L = -0.166415 + j0.102536$ , which was measured separately from CW.

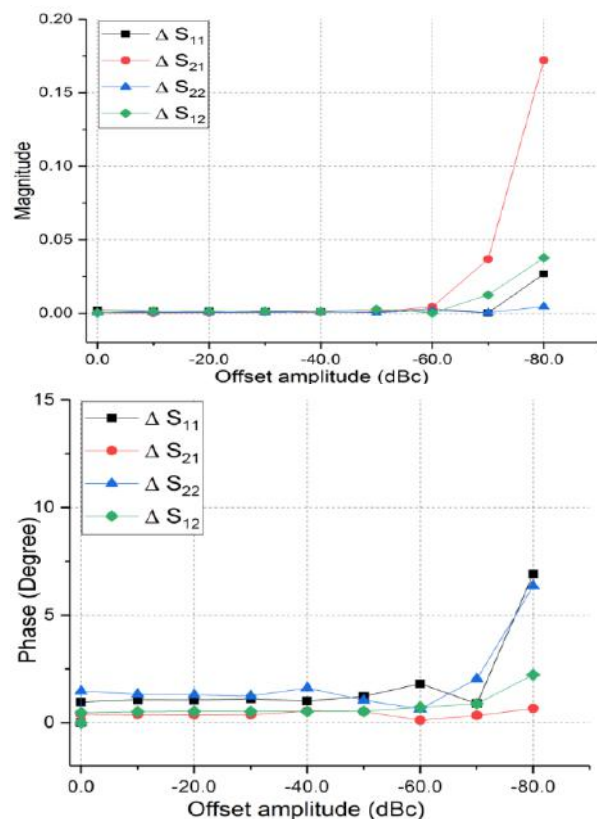


**Fig 3: A comparison of the magnitudes and phases of S-parameters in the main tone and the tickle tone versus the offset amplitude.**

The output impedance of the tickle-tones and harmonics was kept at 50Ohm. Figure 4 shows three different power-offset levels on a CW stepped input power measurements to identify the impact of tickle-tones on the power added efficiency (PAE) of the device. The PAE of each power-offset level was calculated, and then the differences with the PAE of the CW tone were computed individually. It is apparent that offset levels  $\leq -20$ dBc are required to limit the impact on device efficiency to less than 5%.

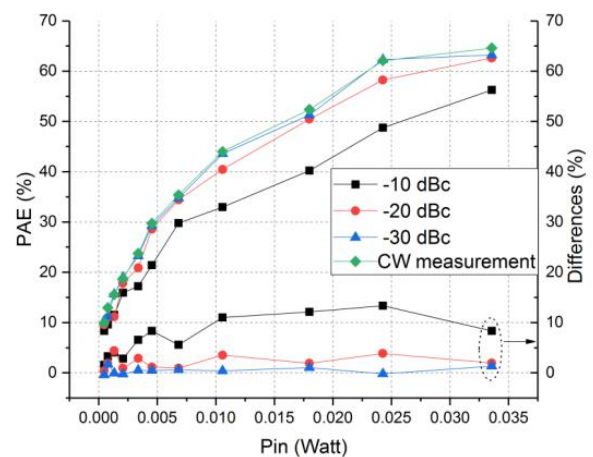


**Fig 4: Different levels of power offsets vs PAE.**

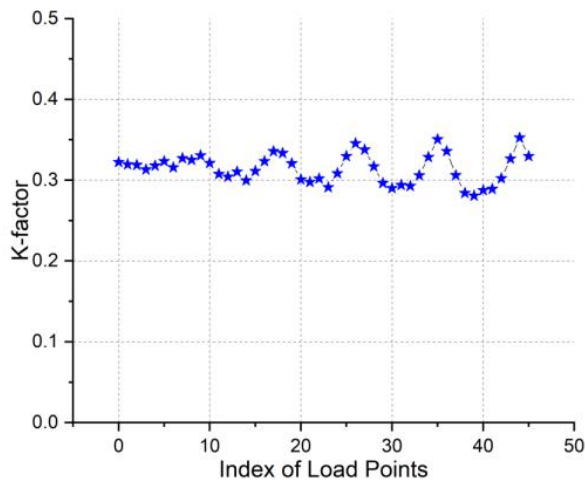
#### 4. Stability Analysis

When reflection coefficient magnitudes exceed unity, oscillation occurs in active circuit elements like transistors. Signals that are reflected are larger than those that are incident. A Smith Chart with negative resistance circles is always outside the unit radius. The effects may only occur because of certain bias conditions, frequency ranges, load impedances, or increased signal levels.

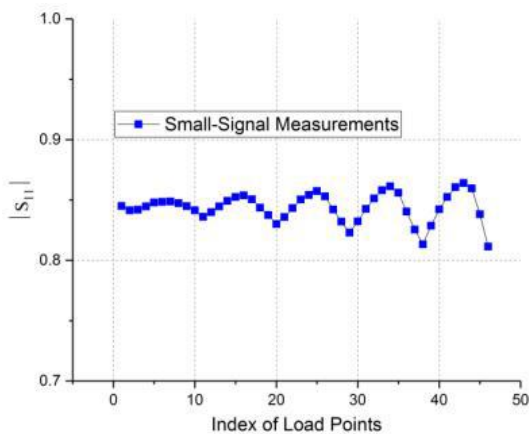
Stability analysis is commonly carried out by computing Rollets stability criteria parameters from DUT S-parameters, [8, 9]. Unconditional stability occurs if  $K > 1$  and  $|\Delta| < 1$ . A potentially unstable condition would be determined by examining it with traditional stability circles [10]. Stability circles mark a border between stable and unstable terminations where load termination stability circles are plotted. It is also possible to analyse the S-parameters determined by tickle tones in relation to load impedance and drive level. In this experiment, the main tone was generated at 1GHz, and the two tones  $T_1$  and  $T_2$  were generated at 100kHz and 250kHz, respectively. Additionally, the tickle-tones were set to -20dBc from the

stimulus, with the large signal input set at 18.95dBm.

According to Figure 5, K-factor values are less than one. Therefore, this measurement is conditionally stable. There can be oscillations at the input port when  $|\Gamma_{in}|$  is greater than 1.0. With  $|\Gamma_{in}| < 1.0$ , the input port is stable, while with  $|\Gamma_{in}| = 1.0$ , it lies on the borderline. Considering the 50Ohm point, it can be determined whether the region inside the stability circle represents stable or unstable termination. As  $|S_{11}|$  for all points is  $< 1.0$  (Figure 6), regions outside the stability circles are stable.



**Fig 5: Load points with different K-factors.**



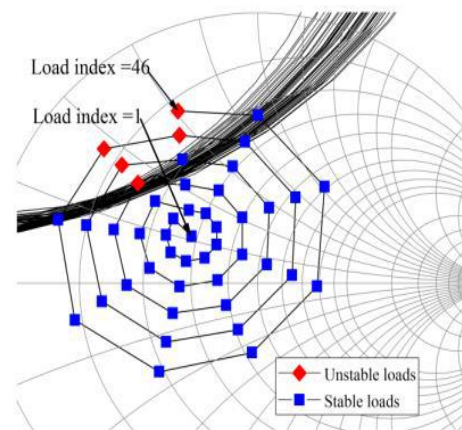
**Fig 6: A small-signal S-parameter is designated by  $|S_{11}|$ .**

Figure 7 illustrates the beneficial knowledge extracted during load-pull measurements regarding stable and unstable loads. It is vital to know this information to avoid designing a PA that would operate in an unstable region or performing measurements that could negatively affect the

measurement system or DUT. Due to the fact that the stability analysis can be performed at each measured load impedance in this case, the Smith Chart shows a high number of stability circles.

A load that is unstable means the  $|\Gamma_{in}| > 1$  (Gamma in represents the true input reflection coefficient for a two-port with arbitrary load termination,  $\Gamma_L$ ) for small-signal measurements. As shown in Figure 8, the input reflection coefficient is calculated using S-parameters for small signals (Tickle tone) and then compared with the reflection coefficient for large signals (Main-tone). In load-pull measurements, there is good agreement between the results, indicating that this approach can be used for useful data extraction.

It is noteworthy that the red colour indicates when  $|\Gamma_{in}| > 1$ ; this indicates that the load may be unstable in Figure 7. Discrepancies between the two measurements



**Fig 7: Stability analysis at each load-point.**

can also be observed, with large-signal measurements indicating an unstable load of seven, while small-signal measurements reflect only a load of five. Discrepancies would increase as load points became denser. Whenever a load is close to the threshold of stability (given by an input reflection coefficient  $|\Gamma| = 1$ ), small-signal S-parameter measurements always give an input reflection coefficient less than large-signal S-parameter measurements. It illustrates the importance of having small-signal measurements with large-signal inputs for monitoring the load stability in real-time.

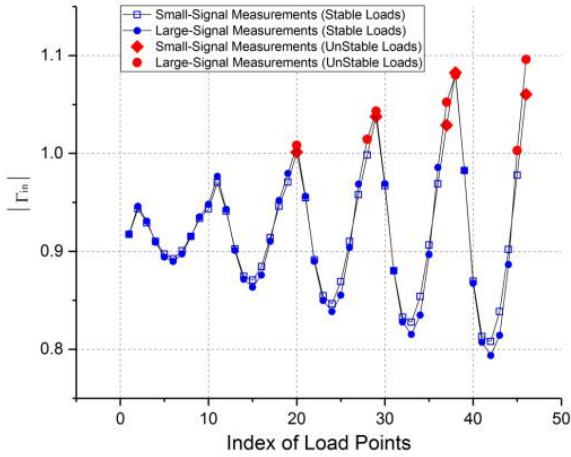


**Fig 8: The index of load points versus  $|\Gamma_{in}|$  for both large and small signals.**

Analysis of the results shows that the calculated power gain (see equation (4)) [11] based on the small-signal 'tickle-tone' parameters matched well with the large-signal parameters. There are points at which the gain cannot be identified when  $|\Gamma_{in}| > 1$ . With the extracted small-signal S-parameters, other gain factors can be calculated without additional costs, such as available gain ( $G_A$ ) and transducer gain ( $G_T$ ), both of which account for the source port mismatch. As a result, because the isolator was imperfect, the  $G_S$  was calculated by measuring the incident and reflected waves of  $T_2$  at port 1.

$$\Gamma_s = \frac{a_{1T2}}{b_{1T2}} \quad \Gamma_L = \frac{a_{2F}}{b_{2F}}$$

$$G_p = \frac{P_L}{P_{in}} = \frac{|S_{21}|^2 (1 - |\Gamma_L|^2)}{(1 - |\Gamma_{in}|^2) |1 - S_{22}\Gamma_L|^2}$$

$$G_A = \frac{P_{avn}}{P_{avs}} = \frac{|S_{21}|^2 (1 - |\Gamma_s|^2)}{(1 - S_{11}|\Gamma_s|^2) (1 - |\Gamma_{out}|^2)}$$

$$G_T = \frac{P_L}{P_{avs}} = \frac{|S_{21}|^2 (1 - |\Gamma_s|^2) (1 - |\Gamma_L|^2)}{|1 - \Gamma_s \Gamma_{in}|^2 |1 - S_{22}\Gamma_L|^2}$$

$$\Gamma_{OUT} = S_{22} + \frac{S_{12} S_{21} \Gamma_s}{1 - S_{11} \Gamma_s}$$

$$\Gamma_{IN} = S_{11} + \frac{S_{12} S_{21} \Gamma_L}{1 - S_{11} \Gamma_L}$$

Equation (3) is marked by subscript  $T_2$  and  $F$ , respectively, which denote load-side second tone and fundamental tone. The ( $\Gamma_s$ ) values are close to 50Ohm impedance as shown in Figure10.

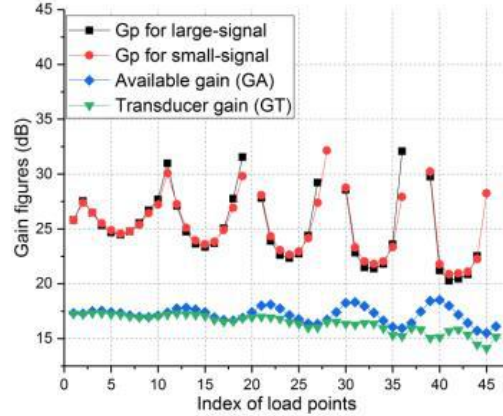


**Fig 9: Different power gain figures for Large and small signals.**

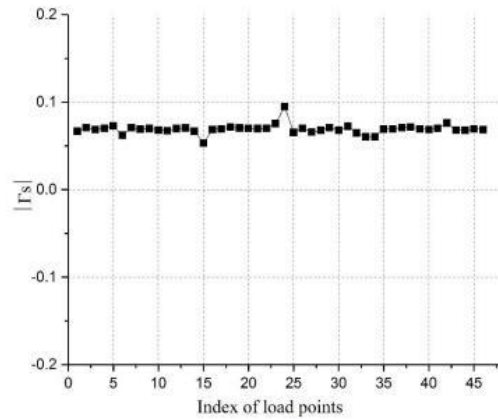


**Fig 10:  $|\Gamma_s|$  at each load impedance point.**

New experiments were conducted to determine the stability of the device at a 50Ohm load with five different power inputs ( $a_1$ ) ranging from 22.7dBm to 4.8dBm while keeping a fixed tickle-tone power output of 2.64dBm as shown in Figure 11.

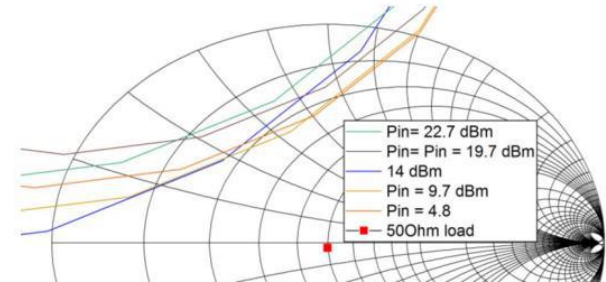


**Fig 11: With various power inputs, stability circles are formed at 50Ohm.**

At the optimum load for maximum output power, the final measurement was performed with the same power input levels. Upon analysis of the results, both measurements showed the unstable region on the Smith Chart was located at the upper left, which indicates that a PA should not be designed inside this region, as it may result in an oscillator design.

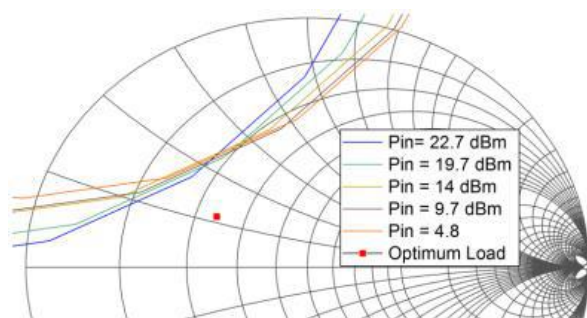


**Fig 12: With different power inputs, stability circles are formed at the optimum load.**

## 5. CONCLUSION

A new approach is presented to extract relevant design data from load-pull measurements in an active load-pull system, using accurate measurements under multi-tone excitation. As a function of both input drive level and output load impedance, S-parameters are obtained by injecting tickle tones, hence a multi-tone stimulus, plus the main tonal stimulus required for classical fundamental load pull. To calculate stability and gain, tickle-tones at -20dBc were found to be sufficient for collecting the required data without distorting the main tone measurements. In the presence of a large-signal input, the system was utilized to measure device S-parameters. By using this approach, it is possible to calculate stability circles and other gain figures in real time while active load-pull measurements are in process.

## 6. REFERENCES

- [1]. Fadhel M Ghannouchi and Mohammad S Hashmi. Load-pull techniques with applications to power amplifier design, volume 32. Springer Science & Business Media, 2012.
- [2]. Mohammad S Hashmi, Fadhel M Ghannouchi, Paul J Tasker, and Karun Rawat. Highly reflective load-pull. IEEE Microwave Magazine, 12(4):96–107, 2011.
- [3]. Mohammad S Hashmi and Fadhel M Ghannouchi. Introduction to load pull systems

and their applications. IEEE Instrumentation & Measurement Magazine, 16(1):30–36, 2013.

- [4]. Thoalfukar Husseini, Azam Al-Rawachy, Johannes Benedikt, James Bel, and Paul Tasker. Automating the accurate extraction and verification of the cardiff model via the direct measurement of load-pull power contours. In 2018 IEEE/MTT-S International Microwave Symposium-IMS, pages 544–547. IEEE, 2018.
- [5]. Ghannouchi, F.M. and M.S. Hashmi, Load-Pull Techniques with Applications to Power Amplifier Design. 2012: Springer Netherlands.
- [6]. Hashmi, M.S., et al., Highly reflective load-pull. IEEE Microwave Magazine, 2011. 12(4): p. 96-107.
- [7]. Hashmi, M.S. and F.M. Ghannouchi, Introduction to load-pull systems and their applications. IEEE Instrumentation & Measurement Magazine, 2013. 16(1): p. 30-36.
- [8]. Rollett, J., Stability and power-gain invariants of linear twoports. IRE Transactions on Circuit Theory, 1962. 9(1): p. 29-32.
- [9]. Platzker, A., W. Struble, and K.T. Hetzler. Instabilities diagnosis and the role of K in microwave circuits. in 1993 IEEE MTT-S International Microwave Symposium Digest. 1993. IEEE.
- [10]. Gilmore, R. and L. Besser, Practical RF Circuit Design for Modern Wireless Systems: Active Circuits and Systems, Volume 2. Vol. 1. 2003: Artech House.
- [11]. Pozar, D.M., Microwave engineering. Wiley, 2012.